Dynamic Climbing of Near-Vertical Smooth Surfaces

Paul Birkmeyer*, Andrew G. Gillies*, and Ronald S. Fearing

***Abstract*— A 10 cm hexapedal robot is adapted to dynamically climb near-vertical smooth surfaces. A gecko-inspired adhesive is mounted with an elastomer tendon and polymer loop to a remote-center-of-motion ankle that allows rapid engagement with the surface and minimizes peeling moments on the adhesive. The maximum velocity possible while climbing decreases as the incline gets closer to vertical, with the robot able to achieve speeds of 10 cm second^{-1} at a 70-degree incline. A model is implemented to describe the effect of incline angle on climbing speed and, together with high-speed video evidence, reveals that climbing velocity is limited by robot dynamics and adhesive properties and not by power.**

I. Introduction

With sensors and electronics continually getting smaller and more capable, mesoscale robots become more viable as highly-functional autonomous mobile platforms. Compared to larger robots, the size of these platforms makes them easy to transport, potentially inexpensive to manufacture, and more capable of navigating cracks and small openings. However, in order for these platforms to be useful in real-world scenarios, they need to be able to traverse different surfaces quickly and efficiently. Previous efforts have developed mesoscale legged robots that run rapidly on horizontal surfaces [1], [2], are highly maneuverable [3], [4], traverse granular media [5], and rapidly climb loose vertical cloth [6].

There are other climbing mesoscale robots, including Climbing Mini-Whegs and Waalbot II; Climbing Mini-Whegs can climb glass vertically and inverted using pressure-sensitive adhesive [7] and WaalBot II has similar capabilities using fibrillar, soft-rubber feet [8]. Larger robots can climb other challenging surfaces, such as RiSE climbing trees and telephone poles [9], [10], StickyBot climbing smooth cabinets and glass [11], and SpinyBot II climbing rough surfaces such as concrete [12]. However, all of these robots are limited to relatively slow velocities and quasi-static gaits. While quasi-static gaits make it easier to guarantee operation within the force limits of an adhesive, dynamic climbing allows faster vertical climbing and reduced power as total mechanical energy fluctuates less and remains close to the potential energy change [13].

DynoClimber and ROCR are prominent examples of rapidly climbing robotic platforms. DynoClimber is capable of climbing at 1.5 body-lengths per second (66 cm/s) and is a novel adaptation of a biologically-derived climbing template [14]; ROCR uses unique tail-swinging dynamics to achieve climbing [15]. However, both robots chose simple climbing surfaces in order to not impede the development and study of their lateral-plane dynamics.

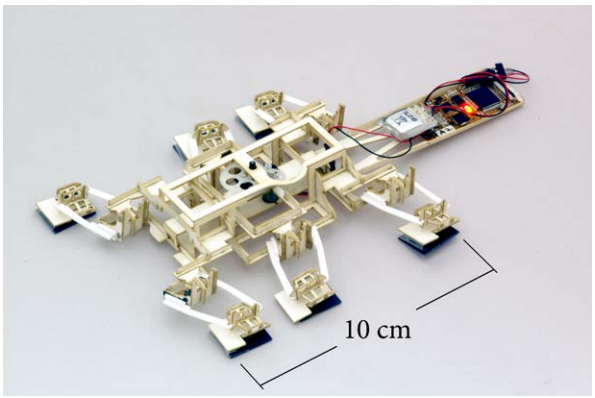

Fig. 1. CLASH equipped with a remote center-of-motion ankle and gecko-inspired adhesive feet.

Previously, the CLASH robot was equipped with a remote-center-of-motion (RCM) joint that allowed it to climb loose vertical cloth at speeds of 15 cm/s, or 1.5 body lengths per second. While climbing a non-rigid surface like cloth is challenging, the penetration-based engagement was simple and straightforward as with ROCR and DynoClimber. This paper presents preliminary designs and results in an effort to adapt CLASH to dynamical climbing of more challenging, smooth surfaces. Here, CLASH uses a gecko-inspired adhesive mounted upon a custom ankle to provide adhesion on a smooth acrylic surface (Figure 1). While dynamic climbing on a smooth vertical surface is not yet possible, the robot is able to climb very steep inclines with rapid velocity. Automated loading tests on the adhesive and feet show that the foot design maintains large shear and adhesive loads through a range of loading angles. The ankle design compensates for unpredictable approach angles and an elastomer tendon is used to transfer the load to the adhesive without generating peeling moments.

II. Design

A. Robotic Platform

CLASH, or Climbing Autonomous Sprawled Hexapod, is a 10 cm robot with a single DC motor that drives all six legs. A tail extends 7.5 cm behind the body and carries the on-board electronics and battery. The body with the electronics, motor, battery and tail have a mass of 15 grams. Adding the

*These authors contributed equally to this work.

This work is supported by the National Science Foundation by Grant EEC-0832819 and Grant 0856789

P. Birkmeyer and R. S. Fearing are with the Department of Electrical Engineering and Computer Science, University of California, Berkeley - {paulb ronf} at eecs.berkeley.edu

A. G. Gillies is with the Department of Mechanical Engineering, University of California, Berkeley - andrew.gillies at berkeley.edu

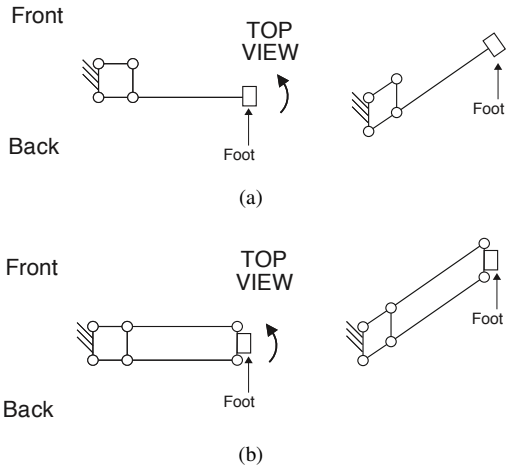

Fig. 2. (a) The claw-equipped CLASH [6] used a traditional oar-like leg that goes through significant yaw deflections during stance. (b) In the new design, a four-bar leg linkage is used to keep the foot oriented parallel to the body and reduce twisting of the adhesive on the surface.

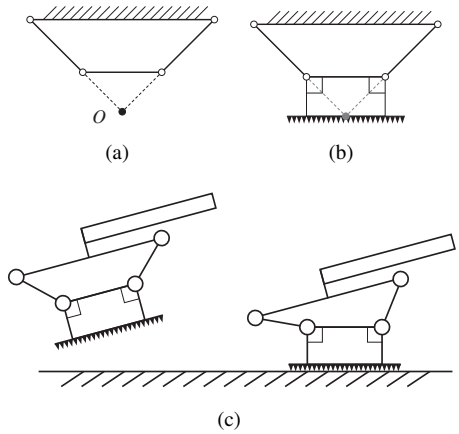

Fig. 3. (a) The ankle is an isosceles-trapezoid four-bar that creates a remote center-of-motion at O. (b) The remote center-of-motion is designed to be at the bottom of the adhesive. (c) This mechanism allows the foot make coplanar contact with the surface and reduces roll peeling moments.

gecko-inspired feet brings the system mass to approximately 19 grams. The robot is constructed using the scaled Smart Composite Microstructure (SCM) manufacturing process in which rigid beams and flexible polymer joints are assembled into mechanisms which define the body, transmission, and kinematics [16]. In CLASH, the single motor drives six hips to create a phase-locked alternating tripod gait. The mechanics of the transmission and resulting hip motions can be seen in [6]. CLASH uses a custom electronics package with 802.15.4 wireless communications to control trials [17].

B. Gecko-Inspired-Adhesive Feet

1) Leg and Ankle Design: The kinematics of the hips in CLASH dictate that the legs move through an elliptical path during locomotion with significant yaw and roll deflections on the legs; relative to the body, the legs yaw during fore-aft swinging and roll when raised and lowered. If an adhesive foot were rigidly mounted to the end of a simple leg as in Figure 2(a), the yaw displacement would result in the adhesive twisting at the ground contact and likely result in failure of the adhesive. To counter this yaw deflection of the foot, a simple parallel four-bar leg structure is introduced. The new leg structure, as seen in Figure 2(b), enforces the constraint that the foot remain parallel with the orientation of the robot.

Figure 3 shows an ankle that allows the foot to roll relative to the leg, enabling the foot to adapt to variable surface angles, body roll, and the changing roll dictated by the kinematics during stance. It is primarily an isosceles trapezoid four-bar mechanism that creates an instantaneous remote center-of-motion (RCM) at point O in Figure 3(a) [18]. The RCM of the ankle is designed to be near the surface of the adhesive (Figure 3(b)). This allows the adhesive to not translate laterally as it is rotates into alignment with the surface. If the center-of-motion were above the surface, the adhesive would have to slide laterally along the surface for the foot to rotate into alignment. Passive alignment without

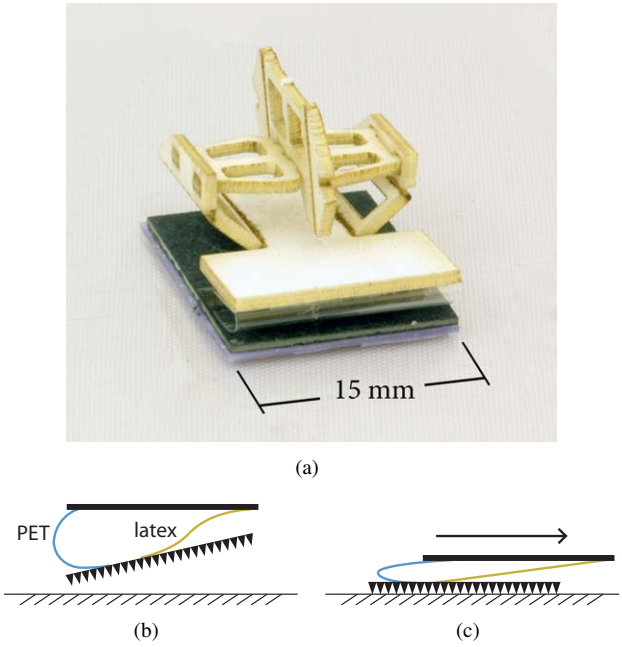

Fig. 4. (a) The gecko-inspired-adhesive foot and RCM ankle joint. (b) The PET loop and latex tendon keep the adhesive constrained to the ankle while unloaded. (c) During stance, the PET loop compresses and unfolds, and the latex tendon transfers the load to the back of the adhesive. The RCM four-bar is removed from (b) and (c) for clarity, but would be attached to the top horizontal beam.

translation is crucial to achieving adhesive engagement. Without an actuated ankle, the work required to do this translation would prevent alignment and engagement of the adhesive.

Another critical reason for the ankle RCM being at the surface is to prevent peeling moments from disengaging the foot during the stroke. Having the ankle rotation axis coplanar with the surface prevents a peeling moment from arising, and therefore full contact is always retained between the foot and the surface [19].

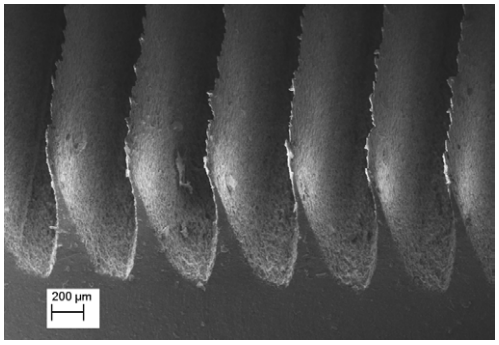

Fig. 5. An image of the gecko-inspired adhesive taken from a scanning electron microscope.

2) Gecko-Inspired Adhesive: Gecko-inspired adhesives have been proposed for use in all-terrain robots due to their ability to adhere to a variety of surfaces in a controllable manner conducive to climbing [20], [21], [22]. Specifically, gecko-inspired adhesives allow for the modulation of normal adhesive force through the application of a shear force, which facilitates easy detachment of the feet at the end of the stroke [23]. Here we implement one such gecko-inspired adhesive in a foot designed for high-speed climbing on vertical surfaces.

The CLASH foot consists of an 18x15 mm pad of micro-fabricated PDMS ridges, using techniques similar to those developed by Sitti [24] and Cutkosky *et al* [25]. A wax engraving tool is used to cut slits in a wax surface. PDMS is then cast into the wax mold. Once cured, the PDMS is peeled from the wax mold, revealing the microridges. The ridges, seen in Figure 5, measure 80 µm wide by 330 µm high, and are spaced 300 µm apart. The adhesive is rigidly mounted on a cardboard backing and attached to the ankle by a thin latex strip and a thin polymer loop, as seen in Figure 4. The latex strip and thin polymer loop are designed so that during loading, the polymer loop complies in the normal and pitch direction in a manner that promotes engagement of the adhesive pad. This normal and pitch compliance work in conjunction with the previously mentioned four-bar ankle to allow the foot to make coplanar contact with the surface.

Once engaged, the adhesive pad is loaded through the latex strip, which is mounted to the center of the adhesive pad, and acts as a tendon in a similar manner to the foot designed by Hawkes *et al* [26]. Under loading, the thin polymer strip unfolds to ensure it does not apply a peel moment to the foot and the latex strip stretches (Figure 4(c)). This stretching is important because due to the dynamics of the running robot, the legs undergo kinematic oscillations and impulses. Without the compliance of the tendon, these rapid kinematic motions would quickly overload the adhesive capabilities of the foot, and the robot would fall. This stretching also allows the robot to catch a slip or arrest a fall by dissipating the fall energy over a larger distance, once again ensuring that the adhesive pad is not overloaded.

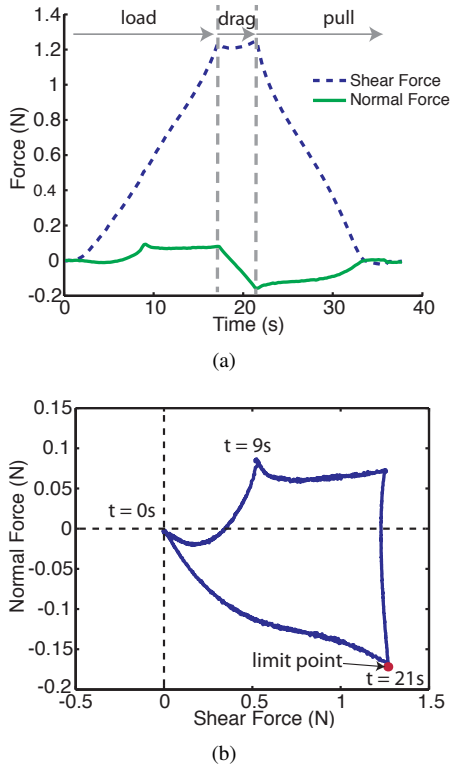

Fig. 6. (a) Force versus time of the gecko-inspired adhesive foot undergoing a load-drag-pull simulated step at 1 mm/s. (b) The same load-drag-pull step in force-space showing the limit point of the gecko-inspired adhesive foot.

III. Results

A. Foot Performance

The foot and gecko-inspired adhesive performance were measured using a custom force displacement apparatus in a manner previously discussed [6]. Adhesive samples were rigidly mounted in 2 sizes (10x10 mm and 15x18 mm) and tested with a simulated load-drag-pull step under displacement control at speeds ranging from 1 mm/s to 20 mm/s. Whole foot-ankle assemblies were also measured with a similar simulated step.

Figure 6(a) shows force vs time for an example trial of one foot. Foot engagment starts with a preload of the patch, followed by dragging the patch into shear. Once the patch is sheared, the foot is pulled to a normal tensile force that will keep the robot adhered to the surface during the stroke. Once the stroke is completed, the shear force is released and the normal force returns to zero, facilitating easy removal of the foot and the end of the stroke.

Figure 6(b) shows the example trial in force-space. Noteworthy is the lowest normal force maintained while under shear. Drawing a line from the origin to this point gives the boundary on the adhesive's performance, which is useful to determine if the feet will be able to hold the robot to the surface. In practice, the foot should be able to maintain contact with the surface as long as loads placed on the foot are within this boundary limit.

Figure 7(b) plots the adhesive limit for a variety of flat mounted adhesive samples and feet, with the best flat samples

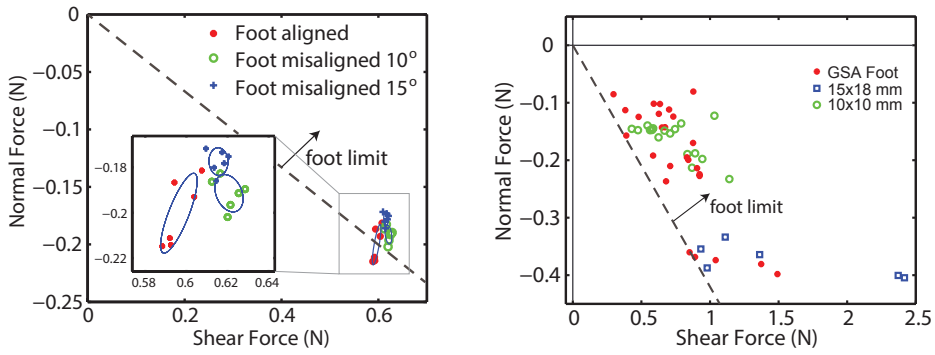

(a) (b)

Fig. 7. (a) A plot of the performance limit of a foot aligned to the test surface and misaligned by 10 and 15 degrees. (b) A plot of the performance limit of 10x10 mm samples (green circle), 15x18 mm adhesive samples (blue plus) and gecko-inspired adhesive feet (red star).

maintaining 0.4 N of tension under 1 N of shear, and the best feet maintaining 0.37 N tensile with 0.9 N shear. The foot design is able to maintain loads far in excess of the robot weight; up to 1 N of shear force compared to 0.19N robot weight, giving a safety factor of 5. This safety factor is critical for rapid climbing, because the adhesive pads must also withstand the dynamic forces of the robot. The adhesive force limit is comparable to forces measured on flat rigidly mounted samples, showing that the foot is able to limit peel moments and misalignments that would otherwise cause the foot to disengage at a lower force. Drag speeds from 1 mm/s to 20 mm/s showed no discernible difference in shear and normal force generation, and these faster velocities are comparable to the foot velocities of CLASH at the steepest inclines tested.

The foot is able to maintain loads even when engaged under a severe roll misalignment of 10 and 15 degrees (Figure 7(a)). Under these misalignments, the generated normal adhesion drops less than 10% from the aligned feet. This again is critical because due to the rapid motion of the legs and variation in the gait, the feet must be able to maintain an adhesive force even under severe misalignment. The companion video demonstrates how the ankle rolls during climbing.

B. Climbing Performance

For the climbing trials with the gecko-inspired adhesive feet, a large plate of smooth acrylic is used as the climbing surface. Starting at an incline of 30 degrees above horizontal and incrementing the angle by 10 degrees, CLASH is operated at a range of frequencies to determine a maximum climbing velocity. The maximum climbing velocity and the stride frequency associated with that velocity are shown in Figure 8. CLASH achieves speeds above 10 cm second^{-1} up to an incline of 70 degrees (Figure 9). Failure to climb an 80-degree incline prompted trials at 75-degree incline to better determine the current limitation of the system. At 75 degrees, CLASH climbs at approximately 1 cm second^{-1}.

Figure 8(a) shows that the maximum velocity decreases approximately linearly as the incline increases. However, the frequencies associated with these velocities have a nonlinear inverse relationship with the incline angle.

While climbing up near-vertical inclines, CLASH exhibits a gait with small aerial phases. Figure 10 shows an aerial phase during 10 cm second^{-1} climb up a 70-degree incline from a high-speed video. To the author's knowledge, this is the steepest robot climbing to exhibit aerial phases or significant sagittal plane dynamics. Even at these fast operating frequencies and aerial phases, the feet provide rapid

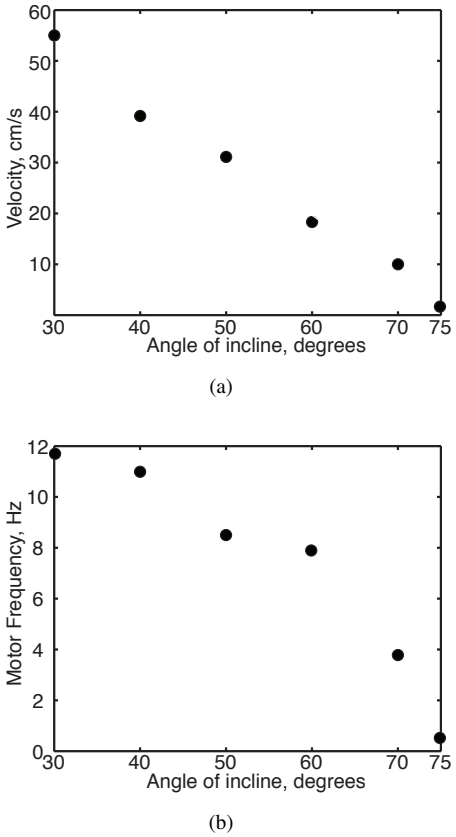

(a)

(b)

Fig. 8. (a) The maximum climbing velocity achieved at a given angle of the smooth acrylic above horizontal. (b) The stride frequency of the robot when it was climbing with the maximum achieved velocity.

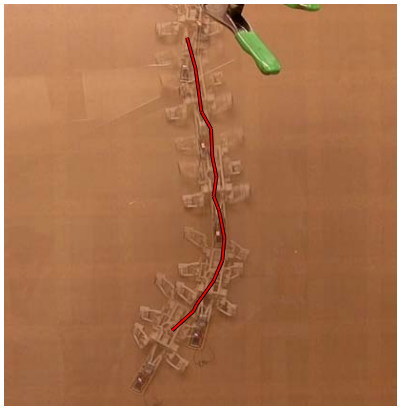

Fig. 9. Superimposed frames of CLASH climbing a 70-degree incline slope at 10 cm second $^{-1}$. The robot had an initial yaw offset but passively corrected its heading during the climb.

reengagement with sufficient adhesion and shear force to continue climbing.

C. Analysis

A simple model of the robot using a spring-mass-damper system (Figure 11(a)) was employed to explain the maximum climbing velocity dependence on surface angle observed in Figure 8(b). We assume that at the instant one tripod leaves the ground, the second tripod is traveling towards the surface with some initial velocity, $\dot{x}_o$, with the mass of robot, m = 0.018 Kg, and stiffness and damping, $k = 5N/m$ and $c = 0.2Ns/m$ representing the overall stiffness and damping of the transmission and legs. The stiffness value calculated for DASH, a similarly constructed and designed robot, was used to estimate the stiffness of CLASH [1]. Using $\tau = \frac{k}{c}t$, $\hat{x} = k^2/gc^2$, $\dot{\hat{x}} = \frac{k}{gc}\dot{x}$ and $\ddot{\hat{x}} = \frac{1}{g}\ddot{x}$ to non-dimensionalize the terms, this system can be described by the following ODE:

$$\ddot{\hat{x}} = -\frac{c^2}{km}\hat{x} - \frac{c^2}{km}\dot{\hat{x}} + cos(\theta) \qquad (1)$$

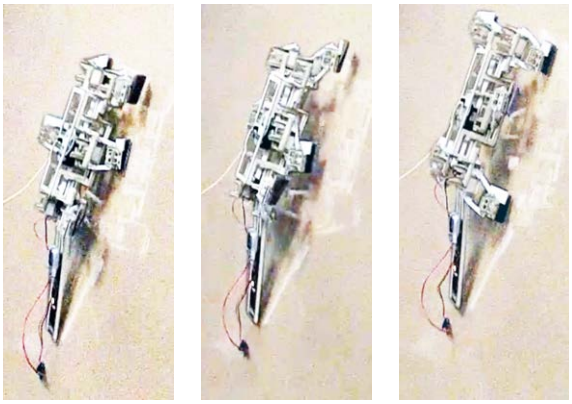

(a) (b) (c)

Fig. 10. Contrast-enhanced frames from high-speed video of CLASH climbing a 70 degree incline at 10 cm second^{-1} showing (a) one leg tripod touching the ground, (b) an aerial phase, and (c) the second leg tripod touching down.

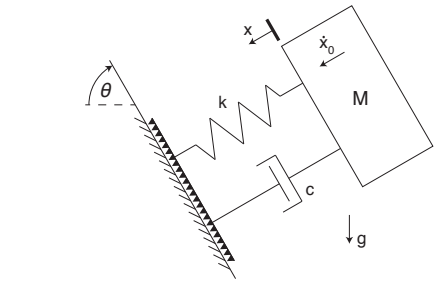

(a)

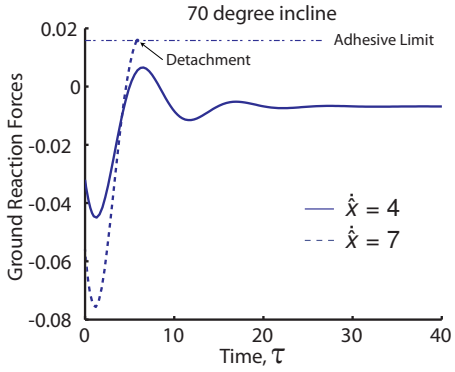

(b)

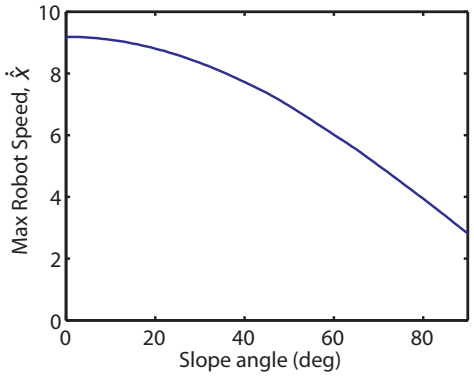

(c)

Fig. 11. (a) Model used showing robot mass, m, and leg stiffness and damping, k and c, at the instant a tripod contacts the ground. (b) Non-dimensionalized impact forces upon touchdown for two different running speeds, with one resulting in loss of contact. (c) Given a certain maximum adhesive force, the climbing velocity, $\dot{\hat{x}}$, must decrease as slope increases in order to maintain contact with the wall.

Once solved, this reveals the well-known damped oscillation seen in Figure 11(b). Of importance for dynamic climbing is the point of maximum outward force on the mass system caused by the robot "bouncing" off the wall. This maximum outward force increases monotonically with the initial inward velocity of the mass, $\dot{x}_o$, which is determined by the overall running speed. If this maximum outward force overcomes the maximum normal adhesion of the feet, they will detach from the wall and the robot will fall. Thus, as the robot velocity increases at a given angle, it will reach a threshold where the robot will bounce and fall off the wall. For the above analysis, a maximum normal adhesive value

of 0.1 N was used, based on data from Figure 7(b).

This threshold is less critical at lower angles, where the component of gravity into the surface is large, and helps to maintain foot contact with the wall. However, as the slope angle increases, the contribution from gravity is reduced, and the threshold is reached at a lower velocity. Figure 11(c) shows that given a certain maximum adhesive force, the climbing velocity must decrease as surface angle increases in order to maintain contact with the wall.

This model also shows the importance of tuning the robot stiffness and damping. If the robot is too stiff or underdamped, the wall reaction forces become much larger, and the adhesive limit is overcome at much lower velocities.

IV. Discussion of Results and Conclusions

Although measured foot adhesion forces should theoretically be great enough to prevent detachment from the wall (Figure 7(b)), it is possible that the normal adhesion is not great enough to prevent pitch-back of the robot during vertical running, as evidenced during running experiments. Our analysis describes one such possible failure, where the impact velocity causes the foot to rebound off the surface. Since higher adhesive strength may prevent this, future foot designs will concentrate on improving the normal force capability of the adhesive. Another possible failure mechanism may be that the dynamics of high-speed running cause alterations in the gait which prevent the feet from properly engaging. This is a more challenging problem that may require more careful tuning of the foot-leg mechanism and more precise tracking data.

In addition to the failure to prevent pitch-back, CLASH could either fail to climb vertically due to either a power limitation or a shear force limitation. The ability of CLASH to rapidly climb vertical loose cloth shows that the robot is not limited by the available power. Also, it does not appear that CLASH is limited by the available shear force. When single feet are mounted to a controlled stage, shear forces approach 1N, more than five times the weight of the robot (Figure 7(a)). When integrated into a climbing robot, the feet generate large shear forces when they rapidly arrest the falling robot on a near-vertical surface, as evidenced in the companion video. The rapid arrest stretches the latex strip, reducing the instantaneous load on the adhesive and often keeping the load within the force limits. The ability of the latex to stretch during loading may also allow load-sharing between the feet, similar to the load sharing within a single foot demonstrated by Asbeck *et al* [12].

CLASH exhibits several interesting behaviors during climbing. CLASH is observed to be stable in yaw; CLASH repeatedly orients itself after a misstep introduces a yaw perturbation. CLASH was designed with most of the mass located toward the rear of the system, including the motor, battery, and electronics to create a stable body pendulum with the center of mass below the center of adhesion [27].

Serial compliance in the transmission is thought to enable the legs to quickly advance their phase and regain purchase if one tripod loses contact suddenly. This occurs because loading the feet creates a phase lag between the motor position and actual leg position due to serial compliance in the transmission. A sudden loss of shear load releases the stored energy and accelerates the legs forward quickly and engages the next tripod sooner than otherwise.

This compliance also has the effect of reducing the stride length as the shear load due to gravity increases with increased incline. This variable stride length may explain why the velocity increases at a faster rate than the motor frequency as incline decreases (Figure 8); with a fixed stride length, they should increase at the same rate.

CLASH has an aerial phase during climbing at inclines up to 70 degrees. Aerial phases are not observed in other climbing robots, including DynoClimber and ROCR which largely ignore motions in the sagittal plane. As CLASH is tuned and adapted vertical surfaces, the authors hope to maintain an aerial or pseudo-aerial phase similar to those seen in geckos [13].

The limitations on stride frequency and thus climbing velocity from the model proposed shown in Figure 11(c) shows a strong behavioral correlation with the observed climbing velocity limitations in Figure 8(b). The actual robot performance does not reach the limitations suggested by the model, likely due to unmodeled phenomena such as transmission dynamics, perturbations from missteps, or asynchronous foot touchdown or pull off. Also, there is an increasing risk associated with loss of contact as the incline increases for which the model does not account. At or near vertical, a failure due to a foot rebounding off of the surface will cause the robot to fail. A foot rebound at lower angles results in intermittent contact and less positive work on the system but is not catastrophic in the same sense.

Future research will use the model to inform the design the next generation of leg and feet designs for dynamic vertical climbing as well as increasing the complexity of the model to better capture other phenomena in the system. The use of an active tail will be explored to achieve controlled heading while climbing, and higher precision tracking with onboard learning will be explored to better tune gaits to given legs and feet.

Acknowledgment

The authors thank A. Birkmeyer for her help with figures. Thanks to A. Pullin for the use of his electronics and N. Kohut for his discussions on dynamics. Thanks also to all the members of Biomimetic Millisystem Lab for their helpful discussions and support.

References

[1] P. Birkmeyer, K. Peterson, and R. Fearing, "DASH: A dynamic 16g hexapedal robot," in *International Conference on Intelligent Robots and Systems (IROS)*, Oct. 2009, pp. 418–419.

[2] A. T. Baisch, C. Heimlich, M. Karpelson, and R. J. Wood, "HAMR3: An autonomous 1.7g ambulatory robot," in *IEEE/RSJ International Conference on Intelligent Robots and Systems (IROS)*, Sept. 2011, pp. 5073 –5079.

[3] A. Hoover, S. Burden, X.-Y. Fu, S. Sastry, and R. Fearing, "Bio-inspired design and dynamic maneuverability of a minimally actuated six-legged robot," in *Biomedical Robotics and Biomechatronics (BioRob), 2010 3rd IEEE RAS and EMBS International Conference on*, Sept. 2010, pp. 869 –876.

[4] A. O. Pullin, N. J. Kohut, D. Zarrouk, and R. S. Fearing, "Dynamic turning of 13cm robot comparing tail and differential drive," in *International Conference on Robotics and Automation (ICRA)*, May 2012.

[5] C. Li, A. M. Hoover, P. Birkmeyer, P. B. Umbanhowar, R. S. Fearing, and D. I. Goldman, "Systematic study of the performance of small robots on controlled laboratory substrates," in *SPIE Defense, Security, and Sensing Conference*, April 2010.

[6] P. Birkmeyer, A. G. Gillies, and R. S. Fearing, "CLASH: Climbing vertical loose cloth," in *IEEE/RSJ International Conference on Intelligent Robots and Systems (IROS)*, Sept. 2011, pp. 5087 –5093.

[7] K. A. Daltorio, T. E. Wei, A. D. Horchler, L. Southard, G. D. Wile, R. D. Quinn, S. N. Gorb, and R. E. Ritzmann, "Mini-Whegs climbs steep surfaces using insect-inspired attachment mechanisms," *Int. J. Rob. Res.*, vol. 28, no. 2, pp. 285–302, 2009.

[8] M. P. Murphy, C. Kute, Y. Menguc, and M. Sitti, "Waalbot II: Adhesion recovery and improved performance of a climbing robot using fibrillar adhesives," *The International Journal of Robotics Research*, vol. 30, no. 1, pp. 118–133, 2011. [Online]. Available: http://ijr.sagepub.com/content/30/1/118

[9] M. J. Spenko, G. C. Haynes, J. A. Saunders, M. R. Cutkosky, A. A. Rizzi, R. J. Full, and D. E. Koditschek, "Biologically inspired climbing with a hexapedal robot," *J. Field Robot.*, vol. 25, no. 4-5, pp. 223–242, 2008.

[10] G. C. Haynes, A. Khripin, G. Lynch, J. Amory, A. Saunders, A. A. Rizzi, and D. E. Koditschek, "Rapid pole climbing with a quadrupedal robot," in *Proceedings of the IEEE International Conference on Robotics and Automation*, 2009.

[11] S. Kim, M. Spenko, S. Trujillo, B. Heyneman, D. Santos, and M. Cutkosky, "Smooth vertical surface climbing with directional adhesion," *IEEE Transactions on Robotics*, vol. 24, no. 1, pp. 65 –74, Feb. 2008.

[12] A. T. Asbeck, S. Kim, M. R. Cutkosky, W. R. Provancher, and M. Lanzetta, "Scaling hard vertical surfaces with compliant microspine arrays," *Int. J. Rob. Res.*, vol. 25, no. 12, pp. 1165–1179, 2006.

[13] K. Autumn, S. T. Hsieh, D. M. Dudek, J. Chen, C. Chitaphan, and R. J. Full, "Dynamics of geckos running vertically," *J Exp Biol*, vol. 209, no. 2, pp. 260–272, 2006.

[14] G. Lynch, J. Clark, and D. Koditschek, "A self-exciting controller for high-speed vertical running," in *IEEE/RSJ International Conference on Intelligent Robots and Systems*, October 2009, pp. 631–638.

[15] S. Jensen-Segal, S. Virost, and W. Provancher, "ROCR: Dynamic vertical wall climbing with a pendular two-link mass-shifting robot," in *IEEE International Conference on Robotics and Automation (ICRA)*, May 2008, pp. 3040 –3045.

[16] A. Hoover and R. Fearing, "Fast scale prototyping for folded millirobots," *IEEE International Conference on Robotics and Automation*, pp. 886–892, May 2008.

[17] S. S. Baek, F. L. Garcia Bermudez, and R. S. Fearing, "Flight control for target seeking by 13 gram ornithopter," in *IEEE/RSJ International Conference on Intelligent Robots and Systems (IROS)*, Sept. 2011, pp. 2674 –2681.

[18] G. Zong, X. Pei, J. Yu, and S. Bi, "Classification and type synthesis of 1-DOF remote center of motion mechanisms," *Mechanism and Machine Theory*, vol. 43, no. 12, pp. 1585 – 1595, 2008. [Online]. Available: http://www.sciencedirect.com/science/article/pii/S0094114X08000050

[19] M. Varenberg, A. Peressadko, S. N. Gorb, E. Arzt, and S. Mrotzek, "Advanced testing of adhesion and friction with a microtribometer," *Review of Scientific Instruments*, vol. 77, no. 6, p. 066105, 2006. [Online]. Available: http://link.aip.org/link/?RSI/77/066105/1

[20] M. K. Kwak, C. Pang, H.-E. Jeong, H.-N. Kim, H. Yoon, H.-S. Jung, and K.-Y. Suh, "Towards the Next Level of Bioinspired Dry Adhesives: New Designs and Applications," *Advanced Functional Materials*, vol. 21, no. 19, pp. 3606–3616, Oct. 2011. [Online]. Available: http://doi.wiley.com/10.1002/adfm.201100982

[21] A. Parness, D. Soto, N. Esparza, N. Gravish, M. Wilkinson, K. Autumn, and M. Cutkosky, "A microfabricated wedge-shaped adhesive array displaying gecko-like dynamic adhesion, directionality and long lifetime." *Journal of the Royal Society, Interface*, vol. 6, no. 41, pp. 1223–32, Dec. 2009. [Online]. Available: http://rsif.royalsocietypublishing.org/cgi/content/abstract/rsif.2009.0048v1

[22] J. Lee, C. Majidi, B. Schubert, and R. S. Fearing, "Sliding-induced adhesion of stiff polymer microfibre arrays. I. Macroscale behaviour." *Journal of the Royal Society, Interface*, vol. 5, no. 25, pp. 835–44, Aug. 2008. [Online]. Available: http://rsif.royalsocietypublishing.org/cgi/content/abstract/5/25/835

[23] N. Gravish, M. Wilkinson, and K. Autumn, "Frictional and elastic energy in gecko adhesive detachment." *Journal of the Royal Society, Interface*, vol. 5, no. 20, pp. 339–48, Mar. 2008. [Online]. Available: http://www.pubmedcentral.nih.gov/articlerender.fcgi?artid=2607396&tool=pmcentrez&rendertype=abstract

[24] M. Sitti, "High aspect ratio polymer micro/nano-structure manufacturing using nanoembossing, nanomolding and directed self-assembly," in *Proceedings 2003 IEEE/ASME International Conference on Advanced Intelligent Mechatronics (AIM 2003)*, vol. 2. IEEE, pp. 886–890. [Online]. Available: http://ieeexplore.ieee.org/xpl/articleDetails.jsp?arnumber=1225459

[25] M. Cutkosky, "Biomimetics and Dextrous Manipulation Lab: Indented Wedges." [Online]. Available: http://bdml.stanford.edu/Main/IndentedWedges

[26] E. W. Hawkes, J. Ulmen, N. Esparza, and M. R. Cutkosky, "Scaling walls: Applying dry adhesives to the real world," in *2011 IEEE/RSJ International Conference on Intelligent Robots and Systems*. IEEE, Sep. 2011, pp. 5100–5106. [Online]. Available: http://ieeexplore.ieee.org/xpl/freeabs_all.jsp?arnumber=6095103

[27] J. E. Clark, D. I. Goldman, T. S. Chen, R. J. Full, and D. Koditschek, "Toward a dynamic vertical climbing robot," in *Proceedings of the 9th International Conference on Climbing and Walking Robots, (CLAWAR '06*, 2006.